Available online at www.sciencedirect.com

ScienceDirect

journal homepage: www.elsevier.com/locate/he

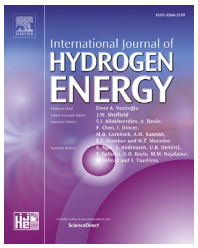

Impact of catholyte recirculation on different 3-dimensional stainless steel cathodes in microbial electrolysis cells

Kyoung-Yeol Kim, Emily Zikmund, Bruce E. Logan [*]

Department of Civil and Environmental Engineering, The Pennsylvania State University, 231Q Sackett Building, University Park, PA 16802, USA

ARTICLE INFO

Article history:
Received 16 August 2017
Accepted 15 October 2017
Available online 6 November 2017

Keywords:
Microbial electrolysis cell
Hydrogen
Stainless steel
Catholyte recirculation
Fermentation effluent

ABSTRACT

While stainless steel (SS) cathodes have shown great promise due to their low cost and high specific surface areas in microbial electrolysis cells (MECs), they have mainly been examined under static (no flow) conditions. Several different SS materials with different 3-dimensional structures (mesh, fiber felt, wool, and brushes) were compared in the absence and presence of fluid flow (0.05, 0.1 and 0.2 cm/s) past the cathode by catholyte recirculation. MECs with wool produced the highest hydrogen production rate with 1.3 ± 0.3 L-H_2/L-reactor/d, which was the same as the Pt control at a catholyte recirculation of 40 mL/min (applied voltage of 0.9 V). In the absence of flow, hydrogen production rates of SS materials decreased by 52% (wool) to 28% (brush). The high hydrogen production rate using wool was likely a result of its high specific surface area (480 m^2/m^3-reactor volume), and reduced cathode overpotential due to gas removal by catholyte recirculation.

Introduction

Hydrogen gas production from cellulose wastes (straw, woodchips, grass residue, paper waste, saw dust, etc.) using dark fermentation can be an effective way to avoid the use of fossil fuels to produce this energy carrier [1]. However, a maximum of only 4 moles of hydrogen can be produced from a mole of hexose by dark fermentation if acetate is the only end product, but practical yields are lower due to the production of other volatile fatty acids (VFAs), alcohols, and bacterial biomass [2,3]. Additional hydrogen production processes are therefore needed to improve hydrogen yields from cellulosic materials [4,5] to increase maximum hydrogen yields closer to the stoichiometric limit of 12 mole-H_2/mole-hexose [6,7].

Microbial electrolysis cells (MECs) can be used to electrochemically produce hydrogen gas at the cathode by using exoelectrogenic bacteria on the anode that can oxidize VFAs and produce an electrical current [8–10]. The favorable anode potential of ~0.3 V (vs. a standard hydrogen electrode, SHE) can reduce the required additional voltage needed to produce H_2 to a minimum of 0.14 V [11]. This cell voltage is much lower than that needed to split water to produce hydrogen gas (1.23 V in theory). Previous studies have shown that acetate and other VFAs, ethanol, and proteins in fermentation effluent can be used to generate the current required to produce hydrogen gas in MECs [12–16]. Coupling an MEC to a dark fermentation process can therefore be an effective method for conversion of biomass into H_2 gas at high yields.

* *Corresponding author.*
E-mail address: blogan@psu.edu (B.E. Logan).
https://doi.org/10.1016/j.ijhydene.2017.10.099

Energy efficient (low overpotential) and inexpensive catalysts are needed to enable the scale up of MECs for practical hydrogen gas or wastewater treatment applications [17]. While Pt is an ideal catalyst for reducing the cathode overpotential, the cost of this metal and the use of expensive binders preclude its use in practical applications. Alternatives to Pt have been proposed for different fuel cell and electrochemical processes, although many of these materials such as molybdenum disulfide (MoS_2) and nickel phosphide (Ni_2P) are appropriate only for highly acidic or alkaline conditions [18,19]. For MEC applications, two of the most promising materials are: stainless steel (SS), which has been tested in various shapes including plates [20], mesh [21], brushes [22], felt [23], and highly porous wool [24,25]; and nickel-based materials, including nickel alloys [26,27], foam [28], and electroformed mesh [29]. SS is particularly promising due to its low cost, good durability, and high electrical conductivity, and certain SS grades such as 304 and 316L also contain a high percentage of nickel (8–14%). Rates of H_2 production in MECs using SS or nickel cathodes can be similar to those obtained using Pt cathodes. For example, H_2 production rate (3.7 ± 0.4 L-H_2/L-reactor/d) using a SS fiber felt cathode (316 SS) [23], or SS brushes (1.7 ± 0.1 L-H_2/L-reactor/d) were shown to be similar to platinum controls [22]. However, these SS materials have only been examined under static electrolyte conditions (no catholyte flow or recirculation). Flow over (or through) a cathode could increase hydrogen gas production since bubbles formed on the electrode surfaces could increase electrode overpotentials and reduce hydrogen gas production rates [30]. Unfortunately, there has been only one study to examine fluid flow past an MEC cathode, and that study used a precious (Pt/Ir) metal oxide, and only very high velocities (1–3 cm/s) which would require high pumping rates and energy consumption. However, recirculation did show reduced overpotentials [31]. The impact of catholyte recirculation on other types of catalyst materials is needed, especially when flow could move within the cathode compared to flow around the cathode. The impact of flow also needs to be compared on both precious and non-precious metal catalysts under exactly the same configurations as the architecture used could complicate comparisons between studies for these different materials.

In this study, we examined for the first time the effect of catholyte recirculation on the performance of four SS materials with very different 3-D structures: mesh, fiber felt, wool, and brushes. Previous tests have not directly compared the performance of these different materials under the same experimental conditions, and none of these materials have been examined under dynamic (flow) conditions. Abiotic electrochemical tests were initially conducted to evaluate performance of the different SS materials at set electrode potentials at different, low catholyte recirculation rates to minimize the energy needed, and compared to a Pt catalyst control to evaluate their performance relative to this well-known precious metal catalyst. These SS materials were then tested in MECs to evaluate H_2 production rates, treatment efficiencies based on chemical oxygen demand (COD) removals, cathodic H_2 recoveries, and energy yields with or without the catholyte recirculation. The costs of these SS materials were evaluated based on projected surface area and total surface area of the materials. A synthetic cellulose fermentation effluent was used as the anolyte in order to provide conditions representative of the performance of an MEC designed to produce hydrogen gas from biomass, with continuous (once through) feeding of the anolyte chamber.

Materials and methods

Cathode materials

Four different cathode architectures were chosen based on their use in other studies for hydrogen gas evolution in the absence of flow [22,23,25,30] (Table 1). SS mesh (304 SS woven wire, 50 × 50 mesh; 8–11% Ni, 18–20% Cr, 2% Mn, 0.08% C, 1% Si, 0.045% P, and 0.03% S; McMaster-Carr) was cut to form a cathode (7 cm × 6.7 cm) with an additional side piece (3 cm × 1.2 cm) to connect the cathode to the circuit (Fig. S2). SS fiber felt (7 cm × 6.7 cm, 88% porosity, BZ100D; Hebei Metal Fibre Science Co. Ltd., CN) and SS wool (SSW, 316L SS, 6 cm × 6.7 cm, thickness 1.5 cm; McMaster-Carr) cathodes were connected to the circuit using additional side piece of SS mesh (4 cm × 1.2 cm) as the current collector for connection to the circuit (Fig. S2). SS brushes were made from 316L SS wires twisted between two 304 SS base wires (5 cm long) forming brushes 1.4 cm in diameter and 2.5 cm long (Gordon Brush Mfg. Co. Inc., CA). The ends of the brushes which extended outside the chamber were used to make the electrical connections. The composition of the 316L SS was assumed to be that of the standard material (10–14% Ni, 16–18% Cr, 0.03% C, 2–3% Mo, 2% Mn, 1% Si, 0.045% P, and 0.03% S) [32].

Pt cathodes (Pt/C), used to benchmark performance, were made as previously described [25]. A mixture of platinum and carbon powder (ETEK C1-10, 10% Pt and Vulcan XC-72) and Nafion (33 mL/cm^2, 5 wt% solution, Aldrich Nafion® perfluorinated ion-exchange resin) was spread on both sides of the 304 SS woven mesh cathode (1 mg/cm^2) described above.

MEC reactor construction and operation

A rectangular two chamber MEC reactor was constructed similar to that previously described [33]. The anode chamber (100 mL) contained 8 graphite fiber brushes with twisted titanium cores (4.5 cm length, 0.8 cm diameter, Mill-Rose, Mentor, OH) closely placed against an anion exchange membrane (Selemion AMV, AGC Engineering Co. Ltd., JP) (Fig. 1). The cathode chamber (68 mL) was re-designed to have the cathodes positioned in the middle of the chamber to allow recirculation flow across both sides of the cathode (Fig. S1). Cathodes were held in place by two Lexan plates cut with an open area of 5.5 cm × 9.5 cm. The side edges of the SS mesh, fiber felt and Pt cathodes were fixed (0.5 cm each side) between silicon gaskets, producing a projected area of 40 cm^2 (Fig. S1). The 5 SS brushes placed in the chamber had a projected area of 17.5 cm^2. The cathode flow chamber had three circular holes at the top and bottom and on one side, so that the catholyte flowed from the bottom on one side, across the cathode chamber, and left on the other side from the top. A reference electrode (Ag/AgCl; model RE-5B, BASi, IN) was inserted through the side hole and sealed with a rubber stopper to monitor the cathode potential. Viton tubing that

Table 1 – Stainless steel (SS) materials used here in MECs. Methods used to estimate the total surface area are provided in the Supporting information.

Cathode	Description	Surface area (cm^2)		Specific surface area[c] (m^2/m^3)		Price ($/$m^2$)	
		Projected	Total	Projected	Total	Projected	Total
SS mesh (SSM)	304SS Woven Wire Cloth	40	80[a]	24	48	46	23
SS fiber felt (SSFF)	SS fiber sintered felt	40	458[a]	24	273	78	7
SS wool (SSW)	Metal 316L pads	40	806[a]	24	480	300	15
SS brushes (SSB)	SS316L wire fill, SS304 base wire	17.5	550[b]	10.4	327	56857	31
Pt cathode (Pt)	Platinum carbon on SS mesh with Nafion binder	40	80	24	48	690	345

[a] Measured by electrochemical technique from Bard & Faulkner (1980) [43].
[b] SS brush 2500 m^2/m^3 from Call et al. (2009) [22].
[c] Cathode surface area per total reactor volume (168 mL).

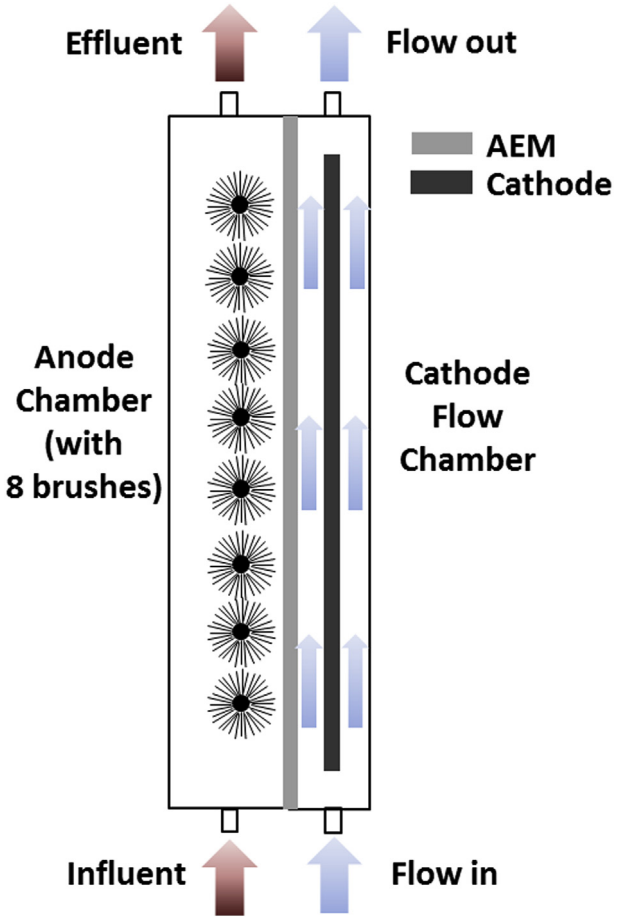

Fig. 1 – A continuous flow MEC design with a cathode recirculation flow.

has a low gas permeability (96412-16, Masterflex) was used to recirculate the catholyte with a peristaltic pump (Model No. 7523-90, Masterflex, Vernon Hills, IL), at flow rates of 20 mL/min (3.4 min hydraulic retention time, HRT; average flow velocity of 0.05 cm/s), 40 mL/min, (1.7 min HRT, 0.1 cm/s), and 80 mL/min (0.9 min HRT, 0.2 cm/s).

The reactor was initially operated as single-chamber microbial fuel cell (MFC) using domestic wastewater (from the primary clarifier of the Pennsylvania State University Wastewater Treatment Plant) as the inoculum and fuel, for a period of 3 months. The cathode was an activated carbon air cathode with a polyvinylidene fluoride (PVDF) diffusion layer [34]. After acclimation, the MFC was switched to MEC mode using a power supply (BK Precision, USA) at an applied voltage of 0.9 V, and fed a synthetic fermentation effluent as the fuel. The synthetic fermentation effluent was prepared as previously described [35], except a phosphate buffer was used instead of bicarbonate buffer. This solution contained sodium acetate (0.27 g), glucose (0.15 g), ethanol (0.11 g), lactic acid (0.07 g), and bovine serum albumin (BSA, 0.32 g) per liter of 50 mM PBS (PBS, Na_2HPO_4: 4.58 g; NaH_2PO_4: 2.13 g, NH_4Cl: 0.31 g; KCl: 0.13 g in 1 L of DI water with mineral and vitamin solutions), for a total COD concentration of 1.2 g/L. The anolyte flow was set at 0.5 mL/min, producing an HRT of 8 h. The catholyte (50 mM PBS without nutrients, 250 mL) was recirculated from a reservoir (250 mL glass bottle) through the cathode chamber, with the bottle sealed gas tight using a rubber cap. Prior to MEC tests, the catholyte was deoxygenated using high purity nitrogen gas (99.998%) for 10 min. A gas collection bag (1 L, Calibrated Instruments, NY) was attached at the top of the glass bottle through the rubber cap to collect gases. Current generation was monitored by measuring voltage across a 10 Ω resistor using a multimeter (Model 2700, Keithley Instruments, Inc., OH).

Electrochemical tests

Electrochemical tests were conducted in an abiotic reactor, using the MEC reactor configuration described above except the anode was a single mixed metal oxide electrode (4.5 cm × 7.5 cm; Rio Grande #335422). Chronopotentiometry (CP) tests were conducted using a potentiostat (VMP3 Workstation, Biologic Science Instruments, USA) with current set for 20 min to achieve a constant cathode potential. Current was increased from 0 to 40 mA in 5 mA increments. Anolyte (50 mM PBS, 250 mL) was recirculated at a rate of 40 mL/min, and the catholyte (deoxygenated) was recirculated at the same flow rates (0, 20, 40, 80 mL/min) used in MEC tests.

Analytical methods and calculations

Gas collected from the gas bag was analyzed for H_2 using a gas chromatograph (Model 8610B, SRI Instruments Inc., USA). The CODs of the influent and effluent solutions were measured

following standard methods (method 5220, HACH company, CO).

The moles of hydrogen that could be produced from the measured current was calculated as $n_{CE} = \int_0^T Idt/2F$, where I is the current (A), F is Faraday's constant (96485 C/mole e^-), and T is the total time. The cathodic hydrogen recovery (r_{cat}, %) was calculated as $r_{cat} = n_{H_2}/n_{CE}$, where n_{H_2} is the mole of hydrogen actually recovered at the cathode [36]. Electrical energy consumption (W_E, J) was calculated as $W_E = \sum_{i=1}^{n}(I_i E_{ps}\Delta t - I_i^2 R_{ext}\Delta t)$, where E_{ps} the applied voltage (V), Δt the time interval, and R_{ext} the external resistance. The energy yield (%, η_E) was calculated using $\eta_E = W_{H_2}/W_E$, where W_{H_2} is the energy in the hydrogen gas produced, based on Gibbs Free energy, as $W_{H_2} = n_{H_2}\Delta G_{H_2}$, where the ΔG_{H_2}=−237.1 kJ/mol and n_{H_2} the H_2 gas produced (mol).

Results and discussion

Electrochemical test with SS materials at different recirculation flow rates

Lower cathode overpotentials were obtained with catholyte recirculation, with little differences in potentials at higher recirculation flow rates (Fig. 2A and B for SSW and Pt controls; other materials shown in Fig. S3). SSW set at a current of 10 A/m^2 had a cathode potential of −1.2 V without catholyte recirculation, but a more positive potential (−0.9 V) was obtained with catholyte recirculation (Fig. 2A). However, cathode overpotentials were not further reduced at higher flow rates of catholyte from 20 to 80 mL/min. The reduction in the cathode overpotentials observed here with flow is consistent with the previous findings using a Pt/Ir mixed metal oxide cathode, where increased flow velocity of the catholyte decreased cathode overpotentials [31], although cathode potentials without flow were not examined in that study.

Among the tested SS materials, similar cathode potentials were obtained for SSW, SSB and SSFF at the catholyte recirculation rates >40 mL/min, but SSM produced more negative potentials than the other SS materials at all flow conditions (Fig. 2). For example, at 10 A/m^2 with a recirculation rate of 40 mL/min, the cathode potentials of SSW (−0.95 V), SSB (−0.93 V) and SSFF (−0.99 V) were quite similar, while the SSM was at least 10% more negative (−1.1 V) (Fig. 2E). More positive cathode potentials for SSW, SSB and SSFF than SSM was likely due to the higher specific surface area of those 3-D SS materials. These abiotic electrochemical tests showed that the SS materials with relatively high specific surface areas (SSFF, SSW, and SSB) could be used to improve hydrogen production compared to that of the SS mesh, and that even low flow rates improved H_2 production rates.

H_2 production rates and current densities of MECs with SS materials

For MEC tests, only the static (no flow condition) and 40 mL/min conditions were tested with the different SS materials due to the small impact of the other flow rates on cathode potentials in the electrochemical tests. With recirculation, the highest hydrogen production rate among the SS materials was obtained with SSW (1.3 ± 0.3 L-H_2/L-d). This rate was the same as that produced using the Pt cathode (1.3 ± 0.1 L-H_2/L-d) (Fig. 3). Similar but slightly lower hydrogen production rates were obtained with SSFF and SSB (1.1 ± 0.1 L-H_2/L-d), while the lowest rate was produced with SSM (0.9 ± 0.1 L-H_2/L-d). H_2 production rates decreased by 28% (SSB) to 52% (SSW) in the absence of catholyte recirculation.

The highest hydrogen production rates by the SSW was likely due to its high specific surface area (806 cm^2 per 40 cm^2 projected area), which was about 10 times higher than that of the SSM and Pt cathodes (Table 1). SSB had a much smaller projected area (17.5 cm^2) than other materials (40 cm^2), but it produced hydrogen production rates similar to the SSFF (458 cm^2) likely also due to its high total surface area (550 cm^2). Current generation was also significantly influenced by the recirculation flow rate, and showed similar trends of an increase with surface area (Fig. 3). Current densities over 110 A/m^3 were produced with recirculation for all SS materials except SSM, which had current densities lower <90 A/m^3. However, current densities with SSW were decreased by 35% without catholyte recirculation, with current densities of all SS materials less than 90 A/m^3 without recirculation. The lower current densities using SSM resulted in the lowest hydrogen production rates among the SS materials.

These results show that hydrogen production rates of SS cathodes could be lower than, or nearly the same as those obtained with Pt catalysts, depending on experimental conditions. For example, with 40 mL/min of recirculation, the H_2 production rate of SSW (1.3 ± 0.3 L-H_2/L-d) was not significantly different from that of Pt (1.3 ± 0.1 L-H_2/L-d, Student's t-test $p = 0.38$) (Fig. 3). However, in the absence of recirculation, H_2 production was significantly lower for SSW than that of Pt ($p = 0.004$). This result for the no-flow tests is similar to that previously reported, where a much lower hydrogen production rate was found using SSW (0.52 L-H_2/L-d) than Pt (1.4 L-H_2/L-d) [25]. The magnitude of the hydrogen production rate here with SSFF was less than that reported in a previous study (3.7 ± 0.4 L-H_2/L-d) using a single-chamber MEC that did not have an ion exchange membrane [23]. It has been previously reported that gas production rates can be increased in single-chamber MECs compared to two-chamber MECs [37]. However, much of the hydrogen gas produced in a single-chamber MEC is converted to methane [38,39], making the use of membrane-less MECs problematic for maximizing hydrogen gas recovery.

Improved hydrogen gas production with catholyte recirculation could be explained by 1) rapidly removing produced hydrogen gas bubble from the electrode surface and 2) reducing the thickness of electrochemical diffusion layer. Hydrogen production can be affected by entrapped hydrogen gas on the cathode surface, as a lower hydrogen production was observed with a higher surface area material (SS mesh) likely due to the high bubble coverage [30]. Cathode overpotential was previously reported to be reduced from −0.3 V to −0.13 V as catholyte flow velocity increased from 1 to 3 cm/s using a Pt/Ir mixed metal oxide cathode [31]. In this study, however, it was shown that much lower velocities of 0.05–0.2 cm/s could be used with SSW, SSFF, and SSB due to

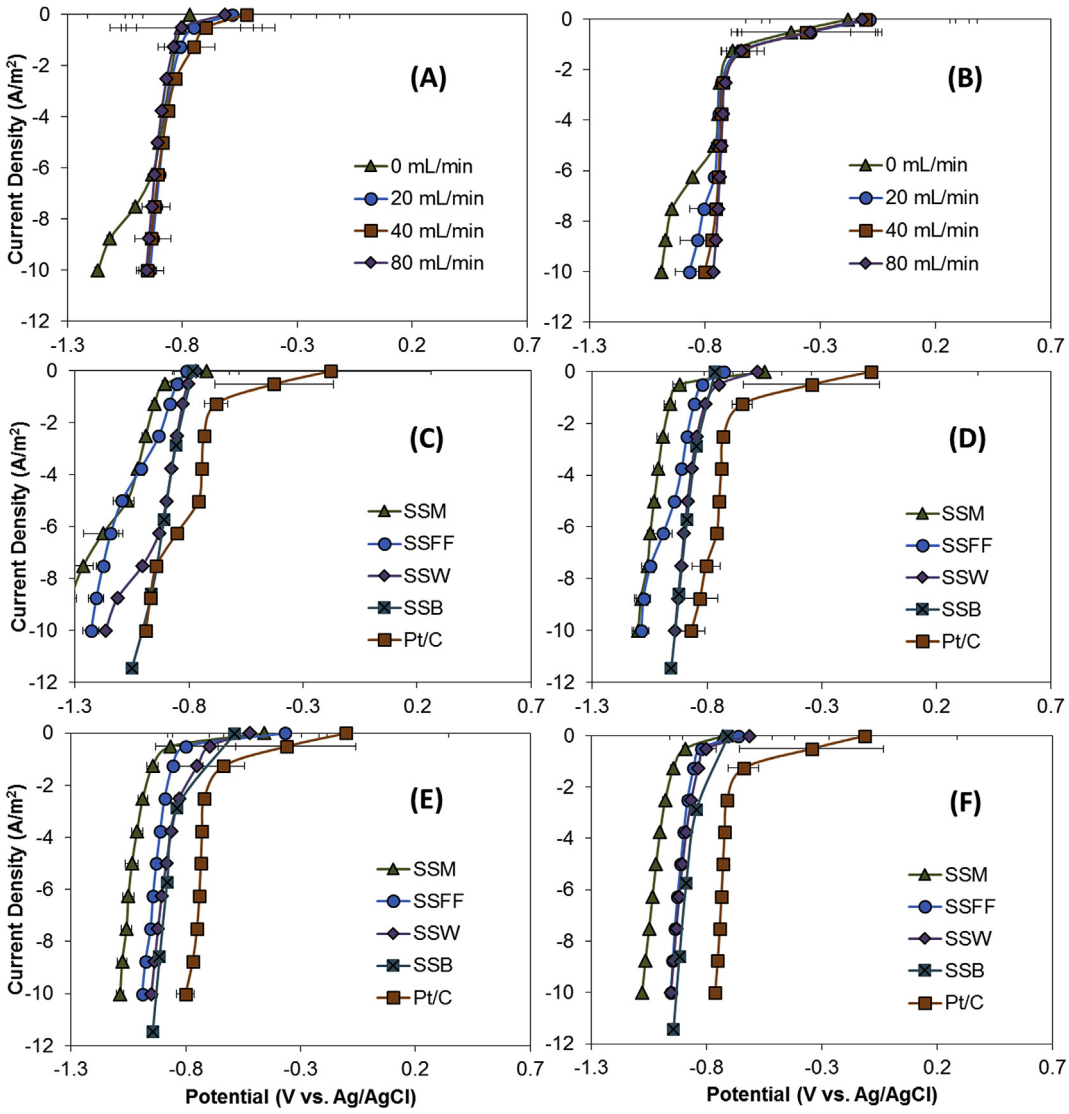

Fig. 2 – Current-potential curves by chronopotentiometry (CP) tests with (A) SSW and (B) Pt cathodes at different flow rates. CP tests with SS mesh (SSM), SS fiber felt (SSFF), SS wool (SSW), SS brushes (SSB) and Pt cathode at different recirculation flow rates: (C) 0 mL/min (no flow), (D) 20 mL/min, (E) 40 mL/min, (F) 80 mL/min. Error bars indicate mean ± SD (n = 3).

their very high surface area compared to the previous flat cathode designs.

H_2 production rates at different applied voltages

Hydrogen production rates were further investigated with SSW at lower applied voltages (0.5 V and 0.7 V), as energy recoveries can be improved. Compared to Pt cathodes, there was a greater decrease in the hydrogen production rate for the SSW at these two lower voltages (Fig. 4). For example, the rate with SSW decreased by 46% between 0.9 V and 0.7 V applied voltage compared to only a 31% decrease for Pt cathodes. Although SSW produced hydrogen at rates comparable to Pt at 0.9 V, lower hydrogen production rates were obtained by SSW at 0.5 V and 0.7 V, likely due to the high overpotential for hydrogen production. Thus, 0.9 V or more would likely be needed for the SSW cathodes to be close to those of Pt cathodes, based on these results in Fig. 4 as well as the electrochemical comparisons in Fig. 2. However, applied voltages above 1.23 V would result in less energy recovery in the hydrogen gas production compared to the electrical power needed for water electrolysis, as 1.23 V is the theoretical voltage needed to split water to produce hydrogen. Also, applied voltages above 1 V have been shown to result in rupture of the cells on the anode in MECs [40].

Cathodic hydrogen recovery and energy efficiency

Cathodic hydrogen recoveries (r_{cat}, %) greater than 95% were obtained in MEC tests with SSW, SSB, and Pt cathodes with catholyte recirculation (Fig. 5A). Much lower recoveries were obtained without catholyte recirculation for the SSW (r_{cat} = 78 ± 3%) and SSB (r_{cat} = 87 ± 5%) cathodes. However, even in the absence of recirculation, the Pt cathode still had a relatively high recovery of r_{cat} = 90%.

Energy yields (η_E, %) were greater than 100% based on the hydrogen gas recoveries in all tests (Fig. 5B). For an applied voltage of 0.9 V, relative to that needed to split water (1.23 V),

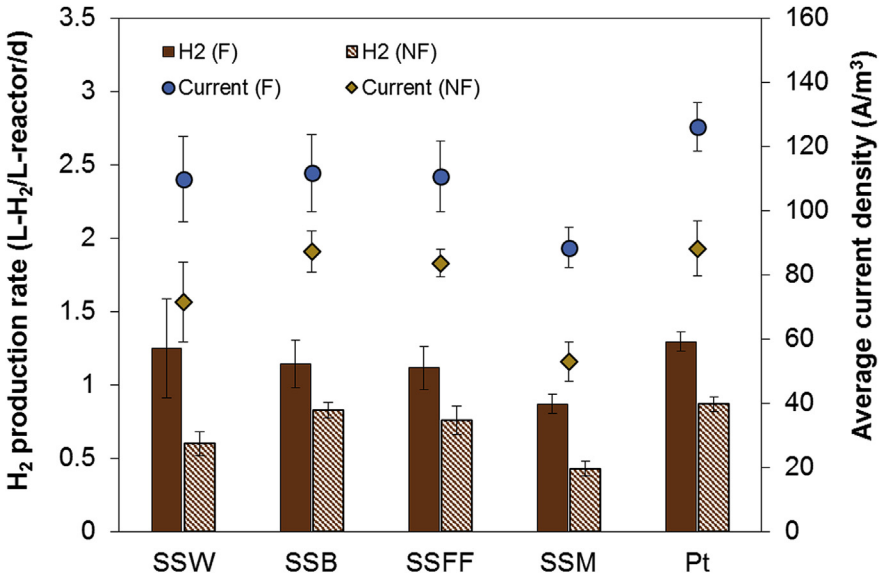

Fig. 3 – Hydrogen production rates (L-H_2/L-d) and current densities (A/m^3) of MECs with SS materials with catholyte recirculation (F, 40 mL/min flow rate) or without recirculation flow (NF, 0 mL/min) (applied voltage of 0.9 V; error bars indicate ± SD, with n ≥ 5).

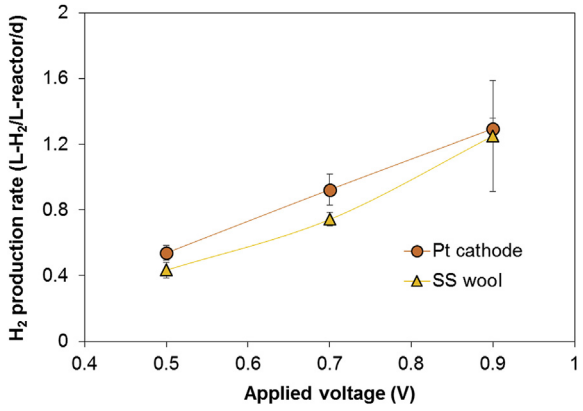

Fig. 4 – Hydrogen production rate (L-H_2/L-reactor/day) of the MEC with SS wool (Pt cathode as control) at different applied voltages (0.5, 0.7 and 0.9 V). Error bars indicate ±SD (n = 3).

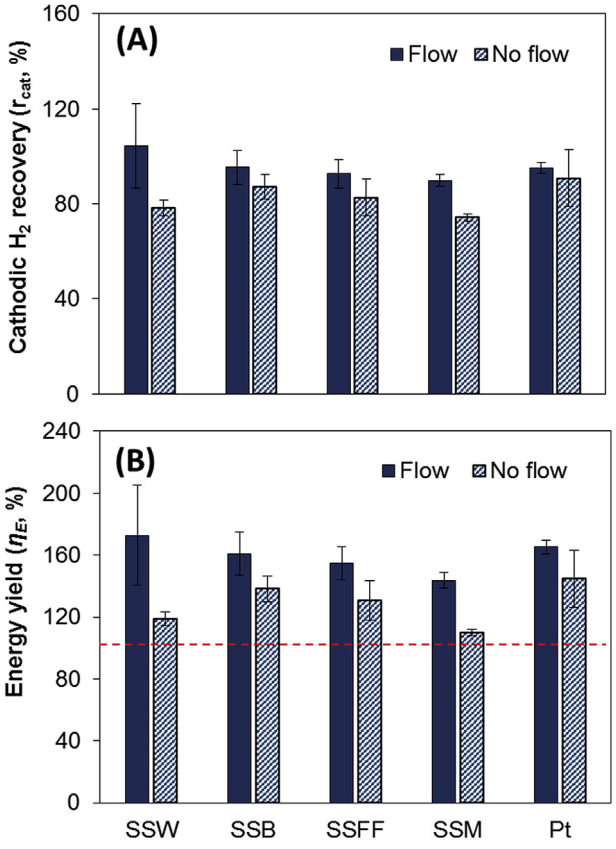

Fig. 5 – (A) Cathodic efficiency (r_{cat}, %) and (B) Energy yield (η_E, energy produced as H_2 per input energy) of the MECs with SS materials with and without recirculation flow at applied voltage of 0.9 V. Red dashed line indicates 100% of energy yield which means produced energy (H_2) is equivalent to energy input (applied voltage). Error bars indicate ±SD (n ≥ 5).

the theoretical maximum energy recovery is η_E=173% [36]. Energy yields here with the SSW and recirculation averaged 173 ± 32% due to the high hydrogen gas recovery efficiencies. Energy efficiencies were only slightly lower for the SSB (161 ± 14%) and Pt (165 ± 5%) with catholyte recirculation. In the absence of recirculation, energy efficiencies decreased to 119 ± 5% for SSW, and 138 ± 8% for SSB (Fig. 5B). Since catholyte recirculation was needed to achieve these high energy yields with the SS materials, energy needed for pumping should also be considered. However, the net energy yields with pumping were only slightly lower (Fig. S5), with SSW decreased for example to 161 ± 31%. The application of lower applied voltages (below than 0.9 V) would likely further increase energy yields, although the hydrogen production rates would also be decreased (Fig. 4).

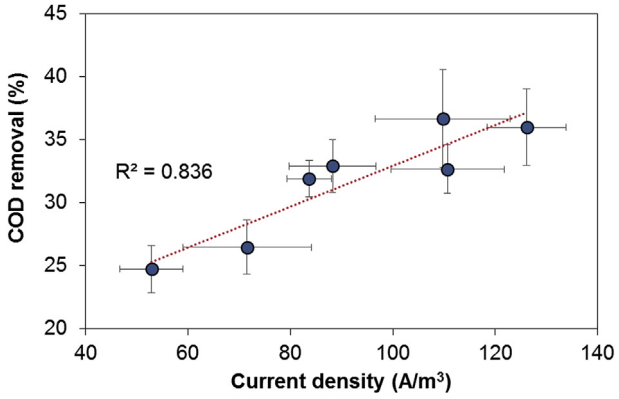

Fig. 6 – COD removal efficiencies (%) according to the current densities (A/m^3) during continuous flow MEC operation in this study. Error bars indicate mean ± SD (n > 5).

COD removal efficiency

With catholyte recirculation, COD removals were in the range of 33–40% for all of the SS cathodes. However, COD removals decreased below 30% without catholyte recirculation. For example, COD removal efficiency with SSW was 37 ± 4% with catholyte recirculation, compared to 26 ± 2% without recirculation. COD removal efficiencies have been shown to be a function of the current densities in MFCs and MECs with higher COD removals reported with higher current densities in an MFC treating high strength wastewater [41]. Regardless of cathode materials, in this MEC study, different current densities with different SS materials or flow conditions were likely more related to COD removal efficiencies (Fig. 6). In order to improve COD removals in MECs, current densities (and hydrogen production rates) would need to be further increased, and the COD removal or hydrogen gas production rates optimized relative to other operational parameters such as HRT and organic loading rates [42].

Conclusions

The highest hydrogen production rate in MEC tests using SS materials was produced using the high surface area SSW (1.3 ± 0.3 L-H_2/L-d) with catholyte recirculation. This hydrogen production rate was comparable to that obtained using a Pt cathode with same conditions. The very high surface area of the SSW (806 cm^2) was likely the most important factor for this result, with the other SS cathodes having a much lower surface areas (80–550 cm^2). For example, the mesh electrodes tested here had the same projected surface area as the other cathodes, but only 80 cm^2 based on the total wire surface area. Catholyte recirculation was critical for obtaining the highest gas production rates, and the energy required for pumping was estimated to be a small loss of energy efficiency. Catholyte recirculation produced higher current densities than static conditions, although the increase was small when the flow velocities were increased from 0.05 to 0.2 cm/s. COD removals of 30–40% could be increased by using longer HRTs and by further improving current densities in the MECs.

Acknowledgements

This work was supported by funds provided by the National Renewable Energy Laboratory (NREL) through the Department of Energy (DOE) CPS Project #21263.

Appendix A. Supplementary data

Supplementary data related to this article can be found at https://doi.org/10.1016/j.ijhydene.2017.10.099.

REFERENCES

[1] Levin DB, Islam R, Cicek N, Sparling R. Hydrogen production by *Clostridium thermocellum* 27405 from cellulosic biomass substrates. Int J Hydrogen Energy 2006;31:1496–503.
[2] Lin P-Y, Whang L-M, Wu Y-R, Ren W-J, Hsiao C-J, Li S-L, et al. Biological hydrogen production of the genus *Clostridium*: metabolic study and mathematical model simulation. Int J Hydrogen Energy 2007;32:1728–35.
[3] Thauer RK, Jungermann K, Decker K. Energy conservation in chemotrophic anaerobic bacteria. Bacteriol Rev 1977;41:100.
[4] Hallenbeck PC, Ghosh D. Advances in fermentative biohydrogen production: the way forward? Trends Biotechnol 2009;27:287–97.
[5] Miyake J, Mao X-Y, Kawamura S. Photoproduction of hydrogen from glucose by a co-culture of a photosynthetic bacterium and *Clostridium butyricum*. J Ferment Technol 1984;62:531–5.
[6] Hawkes FR, Hussy I, Kyazze G, Dinsdale R, Hawkes DL. Continuous dark fermentative hydrogen production by mesophilic microflora: principles and progress. Int J Hydrogen Energy 2007;32:172–84.
[7] Lalaurette E, Thammannagowda S, Mohagheghi A, Maness P-C, Logan BE. Hydrogen production from cellulose in a two-stage process combining fermentation and electrohydrogenesis. Int J Hydrogen Energy 2009;34:6201–10.
[8] Hu H, Fan Y, Liu H. Hydrogen production using single-chamber membrane-free microbial electrolysis cells. Water Res 2008;42:4172–8.
[9] Lu L, Ren ZJ. Microbial electrolysis cells for waste biorefinery: a state of the art review. Bioresour Technol 2016;215:254–64.
[10] Rozendal RA, Hamelers HV, Euverink GJ, Metz SJ, Buisman CJ. Principle and perspectives of hydrogen production through biocatalyzed electrolysis. Int J Hydrogen Energy 2006;31:1632–40.
[11] Zhu X, Yates MD, Hatzell MC, Ananda Rao H, Saikaly PE, Logan BE. Microbial community composition is unaffected by anode potential. Environ Sci Technol 2014;48:1352–8.
[12] Escapa A, Lobato A, García D, Morán A. Hydrogen production and COD elimination rate in a continuous microbial electrolysis cell: the influence of hydraulic retention time and applied voltage. Environ Prog Sustain Energy 2013;32:263–8.
[13] Nam J-Y, Yates MD, Zaybak Z, Logan BE. Examination of protein degradation in continuous flow, microbial electrolysis cells treating fermentation wastewater. Bioresour Technol 2014;171:182–6.

[14] Tuna E, Kargi F, Argun H. Hydrogen gas production by electrohydrolysis of volatile fatty acid (VFA) containing dark fermentation effluent. Int J Hydrogen Energy 2009;34:262–9.
[15] Wang A, Sun D, Cao G, Wang H, Ren N, Wu W-M, et al. Integrated hydrogen production process from cellulose by combining dark fermentation, microbial fuel cells, and a microbial electrolysis cell. Bioresour Technol 2011;102:4137–43.
[16] Lu L, Xing D, Xie T, Ren N, Logan BE. Hydrogen production from proteins via electrohydrogenesis in microbial electrolysis cells. Biosens Bioelectron 2010;25:2690–5.
[17] Rozendal RA, Hamelers HV, Rabaey K, Keller J, Buisman CJ. Towards practical implementation of bioelectrochemical wastewater treatment. Trends Biotechnol 2008;26:450–9.
[18] Hinnemann B, Moses PG, Bonde J, Jørgensen KP, Nielsen JH, Horch S, et al. Biomimetic hydrogen evolution: MoS2 nanoparticles as catalyst for hydrogen evolution. J Am Chem Soc 2005;127:5308–9.
[19] Popczun EJ, McKone JR, Read CG, Biacchi AJ, Wiltrout AM, Lewis NS, et al. Nanostructured nickel phosphide as an electrocatalyst for the hydrogen evolution reaction. J Am Chem Soc 2013;135:9267–70.
[20] Selembo PA, Merrill MD, Logan BE. The use of stainless steel and nickel alloys as low-cost cathodes in microbial electrolysis cells. J Power Sources 2009;190:271–8.
[21] Ambler JR, Logan BE. Evaluation of stainless steel cathodes and a bicarbonate buffer for hydrogen production in microbial electrolysis cells using a new method for measuring gas production. Int J Hydrogen Energy 2011;36:160–6.
[22] Call DF, Merrill MD, Logan BE. High surface area stainless steel brushes as cathodes in microbial electrolysis cells. Environ Sci Technol 2009;43:2179–83.
[23] Su M, Wei L, Qiu Z, Wang G, Shen J. Hydrogen production in single chamber microbial electrolysis cells with stainless steel fiber felt cathodes. J Power Sources 2016;301:29–34.
[24] Heidrich ES, Edwards SR, Dolfing J, Cotterill SE, Curtis TP. Performance of a pilot scale microbial electrolysis cell fed on domestic wastewater at ambient temperatures for a 12 month period. Bioresour Technol 2014;173:87–95.
[25] Ribot-Llobet E, Nam J-Y, Tokash JC, Guisasola A, Logan BE. Assessment of four different cathode materials at different initial pHs using unbuffered catholytes in microbial electrolysis cells. Int J Hydrogen Energy 2013;38:2951–6.
[26] Hu H, Fan Y, Liu H. Optimization of NiMo catalyst for hydrogen production in microbial electrolysis cells. Int J Hydrogen Energy 2010;35:3227–33.
[27] Lu L, Hou D, Fang Y, Huang Y, Ren ZJ. Nickel based catalysts for highly efficient H 2 evolution from wastewater in microbial electrolysis cells. Electrochim Acta 2016;206:381–7.
[28] Jeremiasse AW, Hamelers HV, Saakes M, Buisman CJ. Ni foam cathode enables high volumetric H_2 production in a microbial electrolysis cell. Int J Hydrogen Energy 2010;35:12716–23.
[29] Kadier A, Simayi Y, Chandrasekhar K, Ismail M, Kalil MS. Hydrogen gas production with an electroformed Ni mesh cathode catalysts in a single-chamber microbial electrolysis cell (MEC). Int J Hydrogen Energy 2015;40:14095–103.
[30] Zhang Y, Merrill MD, Logan BE. The use and optimization of stainless steel mesh cathodes in microbial electrolysis cells. Int J Hydrogen Energy 2010;35:12020–8.
[31] Jeremiasse AW, Hamelers HV, Kleijn JM, Buisman CJ. Use of biocompatible buffers to reduce the concentration overpotential for hydrogen evolution. Environ Sci Technol 2009;43:6882–7.
[32] ASTM. Standard Guide for Specifying Harmonized Standard Grade Compositions for Wrought Stainless Steels. Table 1 Chemical Composition Limits, 2008.
[33] Ahn Y, Logan BE. A multi-electrode continuous flow microbial fuel cell with separator electrode assembly design. Appl Microbiol Biotechnol 2012;93:2241–8.
[34] Yang W, Kim K-Y, Logan BE. Development of carbon free diffusion layer for activated carbon air cathode of microbial fuel cells. Bioresour Technol 2015;197:318–22.
[35] Watson VJ, Hatzell M, Logan BE. Hydrogen production from continuous flow, microbial reverse-electrodialysis electrolysis cells treating fermentation wastewater. Bioresour Technol 2015;195:51–6.
[36] Logan BE, Call D, Cheng S, Hamelers HV, Sleutels TH, Jeremiasse AW, et al. Microbial electrolysis cells for high yield hydrogen gas production from organic matter. Environ Sci Technol 2008;42:8630–40.
[37] Call D, Logan BE. Hydrogen production in a single chamber microbial electrolysis cell lacking a membrane. Environ Sci Technol 2008;42:3401–6.
[38] Cusick RD, Bryan B, Parker DS, Merrill MD, Mehanna M, Kiely PD, et al. Performance of a pilot-scale continuous flow microbial electrolysis cell fed winery wastewater. Appl Microbiol Biotechnol 2011;89:2053–63.
[39] Lu L, Xing D, Ren N. Bioreactor performance and quantitative analysis of methanogenic and bacterial community dynamics in microbial electrolysis cells during large temperature fluctuations. Environ Sci Technol 2012;46:6874–81.
[40] Ding A, Yang Y, Sun G, Wu D. Impact of applied voltage on methane generation and microbial activities in an anaerobic microbial electrolysis cell (MEC). Chem Eng J 2016;283:260–5.
[41] Kim K-Y, Yang W, Evans PJ, Logan BE. Continuous treatment of high strength wastewaters using air-cathode microbial fuel cells. Bioresour Technol 2016;221:96–101.
[42] Kim K-Y, Yang W, Logan BE. Impact of electrode configurations on retention time and domestic wastewater treatment efficiency using microbial fuel cells. Water Res 2015;80:41–6.
[43] Bard AJ, Faulkner LR, Leddy J, Zoski CG. Electrochemical methods: fundamentals and applications. New York: Wiley; 1980.